Bažant, Z.P., and Yu, Q. (2010). "Modeling of concrete creep and hygrothermal defor-mations, and computation of their structural effects." *Computational Modeling of Concrete structures* (plenary lecture, EURO-C Conf., Schladming/Rohrmoos, Austria, March 15). N. Bićanić et al., eds., Taylor & Francis, London, pp. 3–13.

Computational Modelling of Concrete Structures – Bićanić et al. (eds)
© 2010 Taylor & Francis Group, London, ISBN 978-0-415-58479-1

Modeling of concrete creep and hygrothermal deformations, and computation of their structural effects

Zdeněk P. Bažant & Qiang Yu
Northwestern University, Evanston, IL, USA

ABSTRACT: This study discusses a physically based formulation of material model for concrete creep and shrinkage, and presents an effective computational approach for structural analysis of creep and shrinkage effects. As an instructive case study, excessive deflections of a prestressed box girder bridge of world-record span, which was built in Palau in 1977 and collapsed after remedial prestressing in 1996, is investigated. A new version of the step-by-step computational algorithm, based on the continuous retardation spectra of compliance curves for different ages at loading, is implemented as a driver program for repeated use of ABAQUS for three-dimensional analysis. The excessive creep deflections are studied by finite element analysis, and their causes are identified. They reveal a need to improve the current standard recommendations of engineering societies. A limited improvement can be achieved by statistical analysis of the existing database from worldwide testing. However, a major improvement will require adopting a model based on the theory of physical processes of creep and shrinkage in the nano-porous structure of cement gel. A model based to a large extent on such a theory is model B3. Its basic features are reviewed.

1 INTRODUCTION

Portland cement concrete is a rather unusual porous material, characterized by both capillary porosity and sub-capillary nano-porosity. The physical and chemical processes in the nano-pores (or gel pores) are believed to be the cause of complex creep properties (Bažant 2001), very different from those of other viscoelastic materials.

The nano-porosity of cement gel has intriguing consequences whose mathematical formulation material model B3 will be reviewed. This model rests on the microprestress-solidification theory (Bažant & Prasannan 1989a,b, Bažant et al. 1997, Bažant et al. 1997), which is a theory that has achieved a unified description of the known creep properties of concrete, including the long-term aging after the hydration process has terminated, the Pickett effect, and the transitional thermal creep.

The purpose of this paper is to summarize (based on a report by Bažant et al. 2007) the lessons from excessive long-time deflections of a record-setting segmentally erected prestressed concrete box girder, discuss the importance of selecting the correct material model for creep and shrinkage, critically comment on the statistical validation of the material model, and review the theoretical physical basis of a realistic material model.

2 EXCESSIVE DEFLECTIONS AND COLLAPSE OF KB BRIDGE IN PALAU

The Koror-Babeldaob (KB) Bridge (Yee 1979, Mc-Donald et al. 2003, Burgoyne & Scantlebury 2006) was built in 1977 in the Republic of Palau, situated in the tropical western Pacific. It connected the islands of Koror and Babeldaob, the former containing the airport and the latter the country capital. As shown in Figure 1a, the main span consisted of two symmetric simultaneously erected cantilevers connected at mid-span by a horizontally sliding hinge. Each cantilever consisted of 25 cast-in-place segments of depths varying from 14.17 m (46.5 ft.) to 3.66 m (12 ft.). The segmental erection of the box girder took about 6–7 months. At the time of completion, the main span of 241 m (790 ft.) set the world record for a prestressed concrete box girder.

In design, the long-term deflection of the bridge was expected to remain in the tolerable range with the final mid-span sag ranging from 0.46 to 0.58 m (18.2 to 23 in.). In the early years, the deflections were benign but then accelerated unexpectedly. After 18 years, the deflection increase measured since the installation of the mid-span hinge that joined the opposite segmentally erected cantilevers reached 1.39 m (54.6 in.) and kept growing (Fig. 1b). If compared to the design camber, an additional creep deflection of 0.22 m (9 in.)

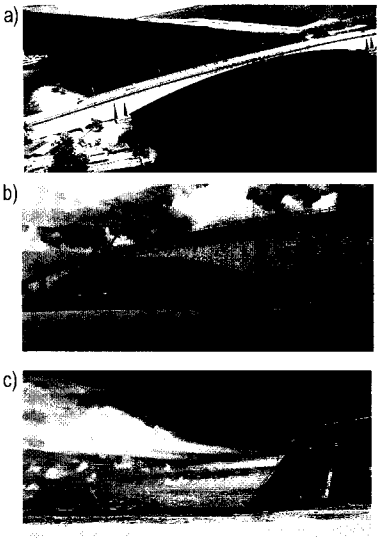

Figure 1. (a) KB Bridge after construction; (b) sag at the mid-span; (c) collapse of KB Bridge.

was accumulated earlier during segmental erection, and so the total deflection was 1.61 m (63.6 in.). The serviceability of the bridge was severely impaired by the excessive deflection, and so a retrofit was carried out in 1996. The mid-span hinge was removed and external prestress within the box was added. Unfortunately, three months later the bridge collapsed (with 2 fatalities and many injuries); see Figure 1c.

After legal litigation in which the deflections and collapse remained unexplained, all the data were sealed in perpetuity. However, on November 6, 2007, the 3rd Structural Engineers' World Congress in Bangalore endorsed a resolution (proposed by the first writer, with the support of many experts) which called, on the grounds of engineering ethics, for the release of all the technical data necessary for analyzing major structural collapses, including the bridge in Palau. The resolution was circulated to major engineering societies. Two months later, the Attorney General of Palau gave his permission to release the technical data. This made it possible to analyze the deflections.

3 NUMERICAL MODELING OF KB BRIDGE

Since structural creep analysis can be broken down to a series of many incremental elastic finite element analyses, which can be most effectively carried out by a commercial general purpose finite element program. The program ABAQUS was selected. Similar to other general purpose programs, ABAQUS is not designed to handle concrete creep. Therefore, a user subroutines that implements the creep integration in time and calls ABAQUS in each time step has been formulated.

Another material subroutine was developed to describe the constitutive model for concrete creep and shrinkage. If all the equations of the constitutive model, converted to a rate form, are put in a proper incremental form, an incremental elastic problem with eigenstrains (or inelastic strains) is obtained for each subsequent time step. The incremental elastic moduli matrices are generally anisotropic and are different for each integration point of each finite element of each time step. So are the eigenstrains, which are non-isotropic.

The incremental elastic relations can be obtained from the differential equation of Kelvin chain model according to the exponential algorithm which is unconditionally stable (Jirasék & Bažant 2002). When the non-aging Kelvin chain model is applied to model B3, one and the same relaxation spectrum, determined in advance, can be used for all the time steps (Bažant & Xi 1995).

Since the cantilevers are symmetric, only one half of the bridge is modelled and simulated. A computational model with 5036 8-node hexahedral elements for concrete and 6764 bar elements for prestressed and unprestressed steel bars is built in ABAQUS; see Figure 2. 316 tendons (Dywidag alloy bars), which are densely packed in up to 4 layers within the top slab, run through the pier. The jacking force of each tendon is about 0.60 MN (135 kips), and the total jacking force at the pier is about 190 MN (42660 kips). The segmental construction sequence, the moving of the formwork traveller and the process of pre-stressing are all reproduced in the simulation by utilizing the functions provided by ABAQUS.

There is no material model in the ABAQUS material library to capture the characteristics of the creep

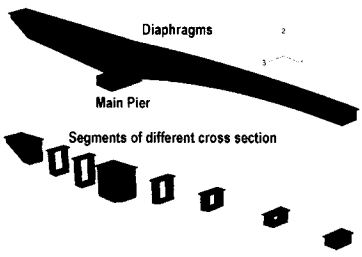

Figure 2. 3-dimensional model of KB Bridge built in ABAQUS.

compliance functions $J(t,t')$ of the creep and shrinkage prediction models used in practice (t = duration of a unit uniaxial stress and t' = age when this sustained stress is applied). Therefore, the appropriate material model has been developed and supplied to ABAQUS. Given the fact that no severe cracking damage was found in the box girders and the observed cracks were sparsely distributed, the concrete of KB Bridge has been assumed as isotropic, characterized by a time-independent Poisson's ratio $\nu = 0.21$ (JICA 1990).

As a compromise between simplicity and accuracy, the creep in concrete is generally considered to follow aging linear viscoelasticity, which implies the principle of superposition in time. The direct application of this principle gives the stress-strain relation in the form of a history integral. However, for the sake of efficiency in large-scale computer analysis, it is advantageous to avoid computation of history integrals. This is made possible by converting the compliance function to an equivalent rate-type form, which has here been based on the Kelvin chain model (Fig. 3).

In model B3, which is based on the solidification theory, the creep is defined for a non-aging constituent of growing volume ($\approx$ cement gel) (Bažant & Baweja 1995, Bažant & Baweja 2000), and in that case the conversion of the compliance function to a rate-type creep law is particularly easy. This can be done according to the solidification theory, in which the aging is taken into account by means of volume growth of the solidifying component, and by a gradual increase with age of the flow term viscosity. This makes it possible to use a non-aging compliance function for the solidifying component, for which one can uniquely determine a continuous retardation spectrum by a simple explicit formula (Widders's formula) for inversion of Laplace transform (Bažant & Xi 1995). The parameters of the Kelvin chain model are in this case constant (i.e., non-aging) and are simply obtained as a discrete representation of the continuous spectrum. For example, if $J(t,t') = \phi C(t-t')$ where ϕ is a non-aging factor, the continuous retardation spectrum can be

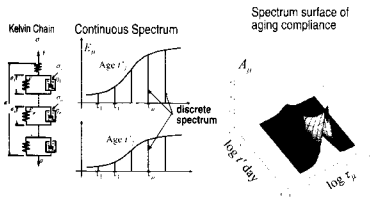

Figure 3. Kelvin chain model and spectrums of non-aging and aging models.

expressed as:

$$A_\mu = \phi(t')L(\tau_\mu)\ln 10\Delta(\log\tau_\mu) \tag{1}$$

$$L(\tau_\mu) = -\lim_{k\to\infty}\frac{(-k\tau_\mu)^k}{(k-1)!}C^{(k)}(k\tau_\mu) \tag{2}$$

where τ_μ is μth retardation time, k is a positive integer, and $C^{(k)}$ represents the kth order derivative of function C ($K \leq 3$ is usually sufficient). In Figure 3, the non-aging spectrum of the basic creep of model B3 is plotted. Note the spectral value A_μ does not diminish as τ_μ increases. The reason is that the basic creep according to model B3 is unbounded.

For empirical models, such as those of ACI (2008), CEB (1990) (or 'fip' 1999), JSCE (1991) and GL (Gardner 2000, Gardner & Lockman 2001), the creep analysis is slightly more complicated since the aging is not separated from the compliance function. Therefore, compliance curves that change with the age at loading must be used. Such a situation was handled in the 1970s by considering the retardation (or relaxation) spectrum to be age dependent, and the age dependence of Kelvin chain elastic moduli was identified from tests data by simultaneous fitting of creep data for various ages at loading. However, the identification problem turned out to be ill-conditioned and the resulting moduli as functions of age non-unique.

As a new simpler approach, one exploits the fact that, during a short time step, compliance function may be considered as age-independent. The continuous retardation spectrum can thus be obtained easily from Eqs. (1) and (2) corresponding to the loading age at each time step, but the spectrum is different for each different age. This continuous retardation spectrum is then approximated by a set of discrete spectral values A_μ ($\mu = 1,2,3,\ldots$), one set for each time step. These spectral values are then used in the individual time steps of the exponential algorithm based on Kelvin chain. No continuous function for $A_\mu(t)$ need be identified and used.

A surface describing the compliance function of ACI for different ages is plotted in Figure 3, with the x-axis representing the retardation time, τ_μ, and the y-axis showing age t'. The disappearance of A_μ at large retardation time τ_μ is due to the fact that the ACI compliance function is (incorrectly) assumed to be bounded.

After obtaining the Kelvin chain moduli, the exponential algorithm, which enables more data and more efficient creep computation, is implemented; see the flowchart in Figure 4. In this algorithm, the stress is assumed to vary linearly in each time step. The initial time steps since the bridge closing at mid-span were 0.1, 1, 10 and 100 days. After that, the time step was kept constant at 100 days up to 19 years.

$$\dot{\gamma}_i(t) + \frac{1}{\tau_i}\gamma_i(t) = \frac{\Delta\sigma}{\Delta t D_j^{(n+1/2)}} \qquad \dot{\gamma}_i(t) = \tau_i \dot{\varepsilon}_i(t)$$

$$\beta_i = e^{-\Delta t/\tau_i} \qquad \lambda_i = \tau_i(1-\beta_i)/\Delta t$$

1. At t = t_0, initialize the internal variables
   $\gamma(0) = 0$
2. For given time step $t_n \rightarrow t_n + 1$
   $D_j^{(n+1/2)}, \beta_i, \lambda_i, E'$
3. Compute the strain increment due to creep
   $\Delta\varepsilon'' = \sum_{i=1}^{m}(1-\beta_i)\gamma_i^{(n)}$
4. For give strain increment, compute the stress increment
   $\Delta\sigma = E'(\Delta\varepsilon - \Delta\varepsilon'')$
5. Update the internal variables
   $\gamma_i^{(n+1)} = \frac{\lambda_i E'}{D_j^{(n+1/2)}}(\Delta\varepsilon - \Delta\varepsilon'') + \beta_i\gamma_i^{n}$

Figure 4. Flowchart of algorithm for creep calculation.

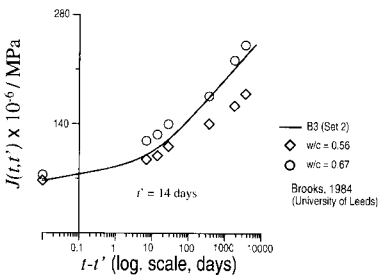

Figure 5. B3 model compared with 10-year creep data by Brooks.

4 COMPARISON OF PREDICTIONS BASED ON DIFFERENT MODELS

For the concrete creep and shrinkage properties, models B3, GL, ACI, CEB (identical to 'fib' 1999) and JSCE are considered and predictions compared. Model B3, in contrast to the others, does not necessarily give a unique prediction because, in addition to concrete design strength, it involves several input parameters depending on the composition of concrete mix, on which there exists no information. These parameters can be set to their default values, but they can also be varied over their plausible range in order to ascertain the range of realistic predictions. The findings are as follows:

1. For model B3, reasonable values of input parameters can be found to match all the measured deflections (as well as the few existing creep tests of duration longer than 10 years; Brooks 1984,2005), while for other models the maximum deflections cannot be approached and the recorded shape of laboratory creep curves cannot be reproduced; see Figure 5.
2. The 18-year deflections calculated by three-dimensional finite elements according the ACI, CEB, JSCE and GL models (with consideration of differential shrinkage and drying creep) are about 66%, 62%, 46% and 53% less than the observed values. On the other hand, the observed deflections are closely matched by calculation on the basis of model B3, provided that model B3 is calibrated to match the 10-year creep tests of Brooks. If the default parameters are used in model B3, its predicted deflection is 43% less than the observed value; see Fig. 6.
3. The bridge in Palau is unique in that the pre-stress loss in grouted tendons was measured by stress relief tests. Three sections of each of three tendons were bared, gages installed, tendons cut and the stress determined from the shortening of the tendon. The result was an average prestress loss of 50%, much larger than the prestress loss of 22% assumed in design. Comparisons of the predictions of various models with the measured prestress loss are shown in Figure 7.
4. The deflection is highly sensitive to prestress loss because it represents a small difference of two large numbers (deflections due to self-weight, and to prestress). According to the ACI, CEB, JSCE and GL models, the prestress loss obtained by the same finite element code is, respectively, about 56%, 52%, 42% and 46% smaller than the measured prestress loss, respectively. Contrarily, the prestress loss predicted by model B3 is very close to what measured in the strain relief tests.
5. Model B3 is in agreement with the measurements if three-dimensional finite elements with step-by-step time integration are used to calculate both the deflections and the prestress losses, and if the differences in shrinkage and drying creep properties caused by differences in slab thickness, temperature and damage are taken into account; Figures 6, 7.
6. The shear lag cannot be neglected. What makes its effect large is that it increases the downward deflection due to self-weight much more than the upward deflection due to prestress.
7. The traditional beam-type analysis, in which the creep and shrinkage properties are assumed to be uniform throughout each cross section, gives grossly incorrect predictions for deflections and prestress loss. These differences can be captured closely by model B3, but poorly or not at all by other models. The compliance function must be determined separately for each slab in the cross section, depending on its thickness and humidity exposure (as well as temperature).

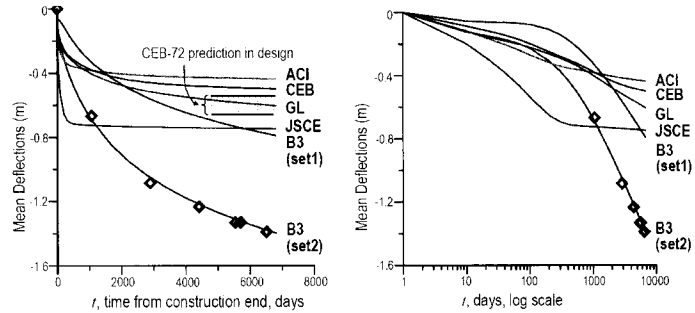

Figure 6. Deflections obtained by B3, ACI, JSCE, CEB and GL models compared with measured. Left: linear scale; right: logarithmical scale.

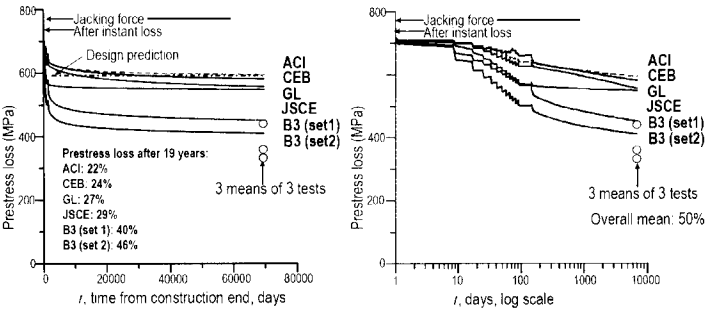

Figure 7. Prestress loss obtained by B3, ACI, JSCE, CEB and GL models compared with the strain relief tests. Left: linear scale; right: logarithmical scale.

8. The results agree with a recent statistical study of Bažant & Li (2009a), which shows that model B3 gives smaller errors in comparison to a comprehensive database than do the ACI, CEB and GL models (whose errors can be of the order of 100%).
9. Creep and shrinkage are notorious for their relatively high random scatter. Therefore, the design should be based on the 95% confidence limits. These limits can be calculated by Latin hypercube sampling of the input parameters analysis.

The reasons why model B3 performs better than the other models can be summarized as follows:

1. A significantly higher long-time creep in model B3, compared to the ACI, CEB and GL models. There are four causes of that: a) theoretical advances on nano-porous materials during the last three decades, incorporated in model B3; b) Model calibration by a larger database, with a rational statistical calibration procedure compensating for the database bias for short times and for small specimen sizes; c) Adjustment of the model to the shape of creep curves observed in individual long-time tests (5 to 30 years), which is obscured when the database is considered only as a whole; and d) rational physical basis of the model.
2. Three-dimensional analysis of deflections and prestress loss, which is much more realistic than the beam bending analysis, especially because it can capture different effects of shear lag on the downward deflection due to self-weight and on the upward deflection due to prestress.
3. Realistic representation of nonuniform shrinkage and drying creep properties in the cross sections, caused by the effect of different wall and slab thicknesses on the shrinkage and drying creep

rates and half-times, as well as by the differences in permeability due to temperature differences (Bažant & Kaplan 1996) and cracking (Bažant et al. 1987).

4. A larger number of input parameters in model B3, which include the water-cement ratio and aggregate-cement ratio. If these parameters are not specified, their variation allows exploring a greater range of responses, compared to the ACI, CEB and GL models. These models are inflexible because of missing these input parameters, and thus provide a unique response for a given design strength of concrete.

Similar conclusions have been obtained by studying the observations in some other large-span prestressed box girders on which sufficient data could be accessed, particularly the Tsukiyono Bridge, Koshirazu Bridge, Konaru Bridge and Urado Bridge in Japan, and the Děcín Bridge in Czech Republic. Together with those bridges, the experience with the KB Bridge in Palau reveals that the current design practice based on empirical creep and shrinkage models and beam-type analysis may lead to dangerous underestimates of the long-term deflections of prestressed large box girders and prestress losses. Improvements in the currently used creep and shrinkage prediction models are, therefore, required.

The improvement needs to based on better statistical evaluation of the existing data. However, the existing data are insufficient by far. Consequently, a physical justification based on the processes in the nano-porous microstructure is vital.

5 MODEL BASED ON PHYSICALLY BASED THEORY AND STATISTICS

Among the existing models, model B3 is the only one with some theoretical foundation—the solidification theory and the theory of microprestress buildup and relaxation in the nano-porous structure of cement gel. The theoretical basis include the following phenomena: 1) process without a characteristic time and asymptotic limit; 2) solidification process; 3) microprestress relaxation; 4) activation energies of creep and hydration; 5) diffusion of water; 6) arguments based on capillarity, surface tension, and free and hindered adsorbed water; 7) cracking or damage; and 8) rate of chemical processes causing autogeneous volume change. After certain idealizations and simplifying hypotheses, consideration of the phenomena led to a compliance function of the form:

$$J(t,t') = q_1 + C(t,t') + C_d(t,t',t_0) \tag{3}$$

$$\dot{C}(t,t') = \left(\frac{q_2}{t^m} + q_3\right)\frac{n\zeta^{n-1}}{1+\zeta^n} + \frac{q_4}{t} \tag{4}$$

where q_1, q_2, q_3, q_4 and n are primary material parameters to be determined from concrete composition, if known; t_0 is the age at the start of drying; $\zeta = t - t'$ = stress duration; $C(t,t')$ is the compliance of basic creep (independent of moisture loss); and $C_d(t,t',t_0)$ is the compliance function of additional creep caused by the drying process (or moisture content change). In model B3, the drying creep and shrinkage strain ϵ_{sh} can be written as:

$$C_d(t,t',t_0) = q_5\sqrt{(e^{-8H(t-t_0)} - e^{-8H(t'-t_0)})} \tag{5}$$

$$\epsilon_{sh}(t,t_0) = -\epsilon_{sh\infty}(1-h_e^3)S(t-t_0)$$
$$= -\epsilon_{sh\infty}(1-h_e^3)\tanh\sqrt{(t-t_0)/\tau_{sh}} \tag{6}$$

where q_5 is material constant; h_e is environmental relative humidity; $\epsilon_{sh\infty}$ is ultimate shrinkage strain determined by the concrete property; τ_{sh} = shrinkage halftime $= k_t(k_s D)^2$, where K_s is the cross section shape factor, D is the effective cross section thickness, k_t is a parameter determined by diffusivity (or permeability); and $H(\hat{t}) = 1 - (1-h_e)S(\hat{t})$.

There is a mathematical reason—the self similarity in time—for which the unbounded individual physical processes involved in creep and shrinkage should be described by power laws, and those that approach a finite bound by decaying exponentials. Eqs. (3) to (6) give a simplified model for practice which approximately describes the mean behavior of a cross section of a slab of thickness D when the bending moment is negligible, i.e., for essentially central in-plane loading.

For a point-wise constitutive model, which can be applied only when the thickness of each slab is subdivided into many finite elements, the solidification-microprestress theory can be characterized by the nonlinear first-order differential equation for the microprestress in the nano-porous structure:

$$\dot{s} + as^2 = c|T\dot{\ln}h| \tag{7}$$

The microprestress s initially produced by the disjoining pressures in nano-pores and by volume mismatch of various constituents relaxes with time at a decaying rate over many years. If there is drying or wetting, or a change of temperature T, the fields of pore humidity h (and temperature) must be calculated for each time step from the nonlinear diffusion equation of drying, and the humidity and temperature change at each integration point of each finite element causes a change in the right-hand side, which produces a build-up of microprestress, and thus an acceleration of creep. The free shrinkage rate $\dot{\epsilon}_{sh} = k_{sh}\,\dot{h}$, at each material point, is proportional to the local pore humidity rate. This is much simpler than the approximate expression in Eqs. (5) and (6) for the overall average shrinkage of

the entire cross section, which includes the approximate effect of the self-equilibrated nonuniform shrinkage stresses and of the cracking that they produce.

Although the form of the constitutive law is physically based, the model B3 parameters have to be obtained by statistical calibration from test data, same as the parameters of purely empirical models. Therefore, statistical study on a large database, is important.

Can the best creep and shrinkage model be identified purely by a standard statistical regression of the existing database? The answer is—no (unless a statistically perfect database were available, which is not the case). In the last several decades, numerous tests have been conducted around the world to investigate the concrete creep and shrinkage. In 1978, the first comprehensive database, consisting of about 400 creep tests and approximately 300 shrinkage tests, was compiled at Northwestern University (Bažant & Panula 1978). A slight expansion based on this database led to what known as RILEM database (Müller & Hilsdorf 1990, Müller 1993, Müuller et al. 1999), which was widely used to calibrate various creep and shrinkage models. Now a significantly expanded database, named the NU-ITI Database, is assembled at Northwestern, comprising 621 creep tests and 490 shrinkage tests (Bažant & Li 2009b).

Although there are thousands of test points in this expanded database, the statistical comparison is useless since the scatter is huge and very little difference can be seen among different models if the entire database is treated as a statistical population (ensemble statistics). The reasons are three: 1) The data points are not sampled uniformly in terms of the loading or drying duration, age of loading, start of drying, and cross section thickness; 2) The scatter caused by various concrete compositions is enormous; and 3) The trends of creep and shrinkage evident from individual tests are obfuscated. Most laboratory test data on creep and shrinkage have durations $\leq$5 years, while the data for 10 to 30 years are very scant (<1% of the total database) and incomplete (Bažant 2000, Bažant et al. 2008). Therefore, steps must be taken to eliminate or minimize the statistical bias before any meaningful statistical comparisons can be made.

As argued in detail in a recent study (Bažant & Li 2009a), it is reasonable to assign the same weight to the total of all test data within each interval of time, size, humidity, and age at loading or start of drying. The subdividion into intervals is based on the regression trend of the corresponding variable. For example, the subdivision of the load duration $t-t'$ is properly made by subdividing the logarithmical scale into equal intervals. Another plague of previous comparisons has been the invention and use of various nonstandard statistical indicators, which violate the principles of statistics. The standard statistical approach—the method of least squares–must be used because it maximizes the likelihood function and is consistent with the central limit theorem. The statistical analysis of the database based proper statistics, with minimized bias, shows that model B3 to provide the best fit.

6 BASIC PHYSICAL PROPERTIES OF CREEP AND SHRINKAGE

As transpired from the numerical modeling of the KB bridge in Palau, the advantages of model B3 over other empirical models arise mainly from its theoretical basis. The nano-porous structure of concrete is the source of creep in hardened Portland cement (Bažant et al. 1997). Creep is most likely caused by separation, slip and restoration of bonds in the calcium silicate hydrates (C-S-H), which is a noncrystalline and strongly hydrophilic material. The weakest bonds are doubtless those crossing the nano-pores of thickness less than about 3 nm.

Except for relative humidities h of water vapor in capillary pores less than about 12%, the adjacent nano-pores are filled with water (Fig. 8a), called the hindered adsorbed water, which gives rise to the so-called disjoining pressure p_d, a concept due to Deryaguin (1955). At 100% humidity, this pressure can reach thousands of atm (or hundreds of MPa). It must be balanced by similarly large tensions (or microprestress) elsewhere in the nano-structure, which are large enough to cause nano-cracks. These tensions obviously promote creep. This explains why the creep is higher at a higher moisture content, provided that the material in thermodynamic moisture equilibrium (a uniform chemical potential in all phases of water).

Concrete, however, hardly ever reaches such equilibrium (at normal temperatures) and, during drying, the opposite is observed—the creep is higher at a lower environmental humidity, which drives the drying. This long discussed and long misunderstood phenomenon is known as the drying creep effect (also called the Pickett effect, or the stress-induced shrinkage).

Since a change of temperature alters the thermal equilibrium, it produces similar phenomena, particularly the transient thermal creep. A change of pore humidity causes a change in disjoining pressure p_d, and thus changes the thickness of the hindered adsorbed water layers and the nano-pores. This is one source of shrinkage ϵ_{sh} (deformation due to a change in humidity at no change in load).

Diffusion (migration) of water molecules along the nano-pores, and in or out of the adjacent capillary pores (>micrometer in size), is one source in the delay of shrinkage and of the part of creep due to drying. But normal structures are so thick that the rate of shrinkage and drying creep of a structure is controlled by diffusion of moisture through structure. This diffusion is highly nonlinear, with the permeability and diffusivity

decreasing about 20-times as the h decreases from 95% to 65%.

Despite this nonlinearity, the drying (weight loss) as well as the shrinkage and drying creep at constant environmental humidity exhibit three basic properties of diffusion processes (Bažant & Xi 1994): a) The drying half-times scale as a square of structure size D (or cross section thickness) (Fig. 8b, c); b) They begin as a square-root function of time (Fig. 8b); and c) They approach the final equilibrium state as a decaying exponential of a power of time (Fig. 8c).

Asymptotic matching of properties b) and c) for shrinkage leads to the tanh-function of the duration (Fig. 8c), normalized by half-time τ_{sh} which is proportional to D^2. A similar function should apply to drying creep compliance J.

Since concretes have thousands of different compositions, it is important to conduct, before design, short-time tests of creep and shrinkage, so as to update the parameters of creep prediction equations (Fig. 8c, d). For creep, which has no upper bound, the update is simple: It suffices to scale the entire creep curve up or down (Fig. 8d). Not so for shrinkage. There is a trap in that the half-time value and the final asymptotic shrinkage value cannot be predicted from short-time shrinkage measurements alone.

An important idea in 1995, which still has not penetrated the practice, is that these values can be easily predicted (by a certain linear regression) if the loss of weight (due to loss of pore water) is simultaneously recorded, and if the total water loss upon heating of the shrinkage specimen at the end of the short-time tests (typically of 1 month duration) is determined. In this manner one can avoid wrong extrapolations shown at lower left and lower right of Fig. 8d.

A convenient property of concrete creep is that, in absence of microcracking, it is linear (within the range of service stresses allowed in structure), i.e., follows the Volterra principle of superposition in time. However there is major complication—the aging. It causes that the creep properties vary significantly with time (at a decaying rate), because of two phenomena: a) the chemical hydration of cement, which lasts at normal temperature for about a year; and b) the gradual relaxation of microprestress in the nano-structure (possibly combined with polymerization of C-S-H), which continues for decades.

The use of microprestress appears indispensable as a unifying concept that captures simultaneously the drying creep (Pickettt effect), the transitional thermal creep and the long-time aging. However, it is not yet clear what is its precise physical mechanism in the C-S-H. Researches at Northwestern University (by H. Jennings) and at M.I.T. (by F.-J. Ulm) may clarify this fundamental question.

The aging causes some thermodynamic restrictions on the formulation of the constitutive equation, which have often been ignored. The easiest way to formulate a thermodynamically legitimate constitute law with aging is to take into account the fact that the newly produced hydrates are deposited on the surface of capillary voids in an unstressed state. Thus aging may be considered as a consequence of the growth of volume fraction $v(t)$ of a certain solidifying constituent (approximately the solid cement gel), which itself is considered to have non-aging properties (Fig. 8e). This represents the essence of the solidification theory, which simplifies the analysis of aging creep in structures.

The absence of aging for the solidifying constituent makes it possible to co-opt the theory of viscoelasticity of polymers, including the rate-type approximation of the non-aging compliance function by a Kelvin (or Maxwell) chain model (Fig. 8e) with an easily obtainable retardation spectrum. This spectral approach avoids the use of history integrals. Also, it is amenable to introducing the effects of variable pore humidity h, temperature T(Bažant et al. 2004) and the softening (Bažant 1995) due to distributed cracking (which cannot be introduced into a Volterra history integral).

Although the Kelvin chain model corresponds to a discrete retardation spectrum, it is better to start with a continuous spectrum. Such a spectrum can be identified from the compliance curve by means of Widder's formula, known from the viscoelasticity of polymers. Discretization of this formula at discrete times, which are best chosen to be spaced by decades in the log-time scale, yields then the Kelvin chain moduli. A direct least-square determination of the Kelvin chain moduli is possible and was used in the 1970s, but it suffers from ill-conditioning and near non-uniqueness. The continuous retardation spectrum is unique, and thus eliminates the problem with ill-conditioning. Besides, its use is computationally more efficient, as demonstrated by the analysis of the KB Bridge in Palau.

The effect of temperature rise on creep and shrinkage is twofold: a) Acceleration of creep, which can be described as a decrease of viscosities of Kelvin units (Fig. 8e) according to the Arrhenius equation, characterized by an activation energy of creep; and b) at the same time an increase in the rate of aging, characterized again by another Arrhenius equation with a different activation energy that governs the rate of hydration. The latter reduces creep. Thus the temperature effect on creep is a competition of accelerating and decelerating influences. For shrinkage it is similar. Temperature increase accelerates diffusion but accelerated hardening hinders shrinkage.

One consequence of ignoring the thermodynamic restrictions due to chemical aging is the condition of non-divergence of the compliance function $J(t,t')$, defined as the strain at time t due to a unit stress applied at age t'; see Fig. 8e. If this condition is ignored, the principle of superposition can produce, after unloading, a recovery reversal (Fig. 8f), and, the relaxation

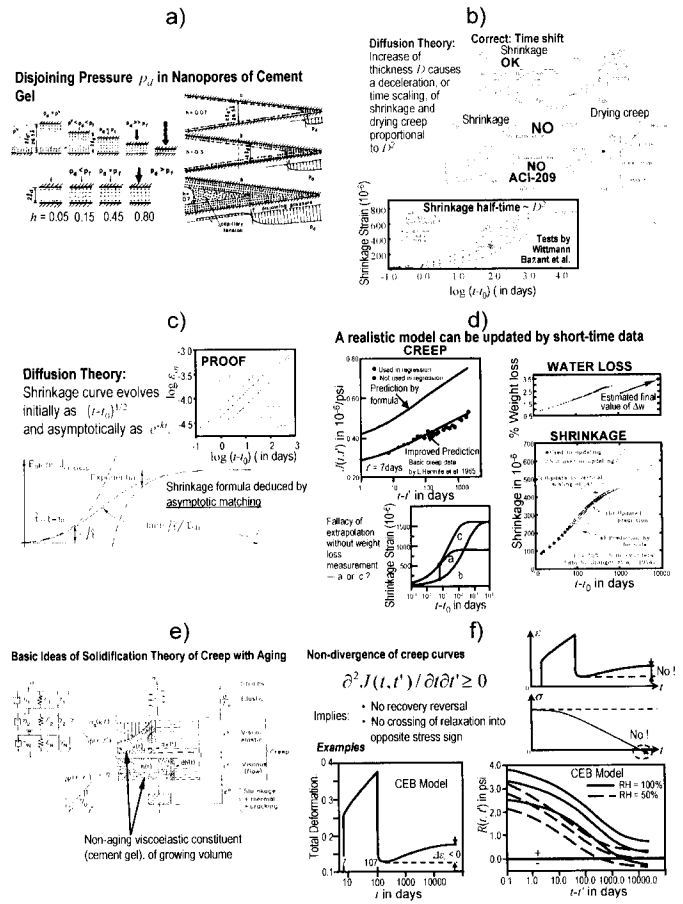

Figure 8. Basic physical phenomena of creep and shrinkage in concrete.

curves at constant strain can cross into the opposite sign. These phenomena violate the second law of thermodynamics if realistic Kelvin or Maxwell chain models with aging are considered (violation, though, need not occur for some contrived rheologic models that give unrealistic compliance curves). Nevertheless, such compliance functions are still used in the design codes of ACI, JSCE and CEB (or 'fib').

The effect of aging on the conventional elastic modulus E (which is really the inverse of compliance function for the duration of about 15 min.) can be greatly simplified by noting that the compliance

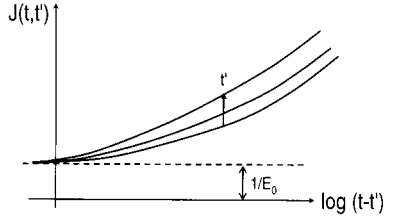

Figure 9. Creep curves for different ages at loading and the asymptotic modulus E_0.

curves for different ages approximately intersect at one point when plotted versus the 0.1-power of stress duration (Fig. 9). The intersection point gives the so-called asymptotic modulus E_0, which corresponds to a fictitious extrapolation of creep curve to the load duration of about 1 ns. With this concept, the compliance function automatically includes the dependence of the conventional elastic modulus $E(t)$ on age t (Fig. 9).

7 CONCLUSIONS

If the advances in research of creep and shrinkage in last three decades were incorporated into the practice, and if the models and methods available today were used at the time of design, the observed deflections of the KB Bridge in Palau would have been expected. This would have forced a radical change of design of this bridge, precluded the fatal retrofit, and thus prevented the final catastrophe. Numerical simulation of the KB Bridge deflections shows that the main causes of error in design are as follows:

1. incorrect compliance and shrinkage functions which are empirically based and rely on a database overwhelmingly dominated by short-term tests ($\leq$3 years duration) and small size tests;
2. neglect of differential shrinkage and drying creep compliance due to a) different thicknesses of cross section walls; b) different temperatures; and c) cracking;
3. lack of three-dimensional analysis. The simplified one- or two-dimensional model leads to inaccurate calculation of shear lags in the slabs and webs;
4. absence of a statistical estimate of the 95% confidence limits;
5. inaccurate time integration and neglect of temperature and cracking;
6. lack of updating of the material parameters by short-time tests.
7. errors in top-bottom differences (a 5% error in prestress can cause a 50% error in the total deflection).

Therefore, design measures that mitigate deflections should be sought. To have a better estimate of long-term deformation in bridge design, the following is necessary:

a. Use a realistic creep and shrinkage model (such as B3 model built on solidification theory);
b. update the model by tests of creep, shrinkage and water loss;
c. analyze the structure three-dimensionally, in time steps; and
d. calculate the 95% confidence limits instead of mean response.

Practical measures can also be undertaken to mitigate the deflections, for example:

a. no mid-span hinge;
b. choice of a concrete with low creep, especially a low long-time creep;
c. use of a higher level of prestress, even so high that an upward deflection is predicted;
d. giving concrete more time to gain strength before prestressing;
e. using stiffer girders of low slenderness; and
f. installing some empty ducts into which additional tendons can be placed later.

Two more points deserve mention: In continuous girders, the deflections are particularly sensitive to tendon layout and can be reduced by the right layout. But a layout benefiting the stress state can at the same time be harmful from the deflection viewpoint. Second, although the absence of a mid-span hinge reduces deflections, excessive deflections may occur, as documented by the Děčín in Bridge.

ACKNOWLEDGEMENT

Financial support from the U.S. Department of Transportation through Grant 0740-357-A222 from the Infrastructure Technology Institute of Northwestern University is gratefully appreciated. Thanks are due to Dr. Khaled Shawwaf of DSI, Inc., Bolingbrook, Illinois, for providing valuable information on the analysis, design and investigations of the bridge in Palau.

REFERENCES

ACI Committee 209. 2008. *Guide for Modeling and Calculating Shrinkage and Creep in Hardened Concrete ACI Guide 209.2R-08*, Farmington Hills.

Bažant, Z.P. 1995. Creep and damage in concrete *Materials Science of Concrete IV*, J. Shalny and S. Mindess, Eds., Am. Ceramic. Soc., Westerville, OH, 355–389.

Bažant, Z.P. 2000. Criteria for rational prediction of creep and shrinkage of concrete. *Adam Neville Symposium: Creep and Shrinkage—Structural Design Effects*, ACI SP-194,

A. Al-Manaseer, ed., Am. Concrete Institute, Farmington Hills, Michigan, 237–260.

Bažant, Z.P. 2001. Creep of concrete. *Encyclopedia of Materials: Science and Technology*, K.H.J. Buschow et al., eds., Elsevier, Amsterdam, Vol. 2C, 1797–1800.

Bažant, Z.P. and Baweja, S. 1995. Creep and shrinkage prediction model for analysis and design of concrete structures: Model B3. *Materials and Structures* 28, 357–367.

Bažant, Z.P. and Baweja, S. 2000. Creep and shrinkage prediction model for analysis and design of concrete structures: Model B3. *Adam Neville Symposium: Creep and Shrinkage—Structural Design Effects*, ACI SP-194, A. Al-Manaseer, ed., 1–83. (update of RILEM Recommendation published in *Materials and Structures* Vol. 28, 1995, 357–365, 415–430, and 488–495).

Bažant, Z.P., Cusatis, G. and Cedolin, L. 2004. Temperature effect on concrete creep modeled by microprestress-solidification theory. *J. of Eng the Mechanics ASCE* 130 (6) 691–699.

Bažant, Z.P., Hauggaard, A.B. and Baweja, S. 1997. Microprestress-solidification theory for concrete creep. II. Algorithm and verification, *J. of Engrg. Mech. ASCE* 123(11), 1195–1201.

Bažant, Z.P., Hauggaard, A.B., Baweja, S. and Ulm, F.-J. 1997. Microprestress-solidification theory for concrete creep. I. Aging and drying effects, *J. of Engrg. Mech. ASCE* 123(11), 1188–1194.

Bažant, Z.P. and Kaplan, M.F. 1996. *Concrete at High Temperatures: Material Properties and Mathematical Models*, Long-man (Addison-Wesley), London (2nd printing Pearson Education, Edinburgh, 2002).

Bažant, Z.P. and Li, G.-H. 2009a. Unbiased statistical comparison of creep and shrinkage prediction models. *ACI Materials Journal*, 106(6), 610–621.

Bažant, Z.P. and Li, G.-H. 2009b. Comprehensive database on concrete creepa and shrinkage. *ACI Materials Journal*, 106(6), 635–638.

Bažant, Z.P., Li, G.-H. and Yu, Q. 2008. Prediction of creep and shrinkage and their effects in concrete structures: critical appraisal. *Proc., 8th International Conference on Concrete Creep and Shrinkage (CONCREEP-8)*, Ise-Shima, Japan, T. Tanabe et al. eds., CRC Press/Balkema, 1275–1289.

Bažant, Z.P. and Panula, L. 1978. Practical prediction of time-dependent deformations of concrete. Part I: shrinkage. Part II: creep. *Materials and Structures*, 11(65), 307–328.

Bažant, Z.P. and Prasannan, S. 1989a. Solidification theory for concrete creep: I. Formulation. *Journal of Engineering Mechanics ASCE* 115(8), 1691–1703.

Bažant, Z.P., and Prasannan, S. 1989b. Solidification theory for concrete creep: II. Verification and application *Journal of Engineering Mechanics ASCE*, 115(8), pp. 1704–1725.

Bažant, Z.P., Şener, S. and Kim, J.-K. 1987. Effect of cracking on drying permeability and diffusivity of concrete. *ACI Materials Journal*, 84, 351–357.

Bažant, Z.P. and Xi, Y. 1994. Drying creep of concrete: Constitutive model and new experiments separating its mechanisms. *Materials and Structures*, 27, 3–14.

Bažant, Z.P. and Xi, Y. 1995. Continuous retardation spectrum for solidification theory of concrete creep *J. of Engrg. Mech. ASCE* 121(2), 281–288.

Bažant, Z.P., Yu, Q. and Li, G.-H., Klein, G., and Křístek, V. (2007). "Explanation of excessive long-time deflections of collapsed record-span box girder bridge in Palau", *Prelim. Structural Engrg. Report 08-09/A222e*, Infrastructure Technology Institute (ITI), Northwestern University.

Brooks, J.J. 1984. Accuracy of estimating long-term strains in concrete. *Magazine of Concrete Research*, 36(128), 131–145.

Brooks, J.J. 2005. 30-year creep and shrinkage of concrete. *Magazine of Concrete Research*, 57(9), 545–556.

Burgoyne, C. and Scantlebury, R. 2006. Why did Palau bridge collapse? *The Structural Engineer*, 30–37.

CEB-FIP Model Code 1990. *Model Code for Concrete Structures*. Thomas Telford Services Ltd., London, Great Britain; also published by Comité euro-international du béton (CEB), Bulletins d'Information No. 213 and 214, Lausanne, Switzerland.

Deryagin, B.V. 1955. The definition and magnitude of disjoining pressure and its role in the statics and dynamics of thin fluid films, *Kolloid Zh.* 17, 205–214.

FIB 1999. *Structural Concrete: Textbook on Behaviour, Design and Performance, Updated Knowledge of the CEB/FIP Model Code 1990*. Bulletin No. 2, Federation internationale du béton (FIB), Lausanne, Vol. 1, 35–52.

Gardner, N.J. 2000. Design provisions of shrinkage and creep of concrete *Adam Neville Symposium: Creep and Shrinkage- Structural Design Effect* ACI SP-194, A. AlManaseer, eds., 101–104.

Gardner, N.J. and Lockman, M.J. 2001. Design provisions for drying shrinkage and creep of normal strength *ACI Materials Journal* 98(2), Mar. Apr., 159–167.

Japan International Cooperation Agency (JICA). 1990. *Present Condition Survey of the Koror-Babelthuap Bridge*, Feburary, 42 pages.

Jirásek, M. and Bažant, Z.P. 2002. *Inelastic analysis of structures*, John Wiley & Sons, London and New York.

JSCE 1991. *Standard Specification for Design and Construction of Concrete Structure*, Japan Society of Civil Engineers (JSCE), in Japanese.

McDonald, B., Saraf, V. and Ross, B. 2003. A spectacular collapse: The Koro-Babeldaob (Palau) balanced cantilever pre-stressed, post-tensioned bridge *The Indian Constrete Journal* Vol. 77, No.3, March 2003, 955–962.

Müller, H.S. 1993. Considerations on the development of a database on creep and shrinkage tests. *Creep and Shrinkage of Concrete*, Proceedings of the 5th International RILEM Symposium, Barcelona, Spain, Bažant Z.P. and Carol I., eds., E&F Spon, London, UK, 859–872.

Müller, H.S., Bažant, Z.P. and Kuttner, C.H. 1999. Database on creep and shrinkage tests. *RILEM Subcommittee 5 Report*, RILEM TC 107-CSP, 81 pages.

Müller, H.S. and Hilsdorf, H.K. 1990. *Evaluation of the Time-Dependent Behaviour of Concrete: Summary Report on the Work of the General Task Force Group No. 199*, Comité Euro-Internationale du Béton, Lausanne, Switzerland, 201 pages.

Pickett, C. 1942. The effect of change in moisture-content on the creep of concrete under sustained load. *ACI J.* 38, 333–356.

Yee, A.A. 1979. Record span box girder bridge connects Pacific Islands *Concrete International* 1 (June), 22–25.